

Evaluation of Nonlinear Distortion in ADCs Using Multisines¹

Pedro Cruz*, Nuno Borges Carvalho* and Kate A. Remley[†]
 *Instituto de Telecomunicações – Universidade de Aveiro – Portugal
 †National Institute of Standards and Technology, Boulder, CO, USA

Abstract—This paper characterizes nonlinear distortion in an analog-to-digital converter (ADC) when excited by representative communication signals having non-constant time-domain envelopes. The effect of subjecting the ADC to signals that present a range of values of peak-to-average power ratio is studied in order to understand the impact of various nonlinear ADC mechanisms in the transmission chain.

Index Terms—analog-to-digital converter, nonlinear distortion, nonlinear measurements, nonlinear models, software defined radio.

I. INTRODUCTION

WE analyze the effect of non-constant envelope excitation on various nonlinear mechanisms present in analog-to-digital converters (ADCs). The nonlinearity of an ADC limits the maximum value of signal-to-noise ratio (SNR)—and thus sensitivity—of a given wireless system [1-2]. ADCs are inherently nonlinear because they directly convert an analog signal to discrete values. Several mechanisms may distort the signal in this process, some of which depend on the peak value of the input signal. In fact, a recent study [3] showed that the peak-to-average power ratio (PAPR) of the excitation is a main limitation of the ADC component.

Recent advances in ADC fabrication and design allow RF signals to be converted to the digital domain immediately without the need for any further frequency down-conversion. Commercially available ADCs are now available that operate at frequencies in the gigahertz range which enables the evolution of the software defined radio concept [4] where RF signals covering a wide range of frequencies and modulations are digitized.

However, the approach for characterizing ADCs in existing standards documents is primarily devoted to low frequency and static approximations of the ADC itself. There are two main standards that are related to ADC characterization: IEEE Standard 1241-2000 [1], (IEEE Standards for Terminology and Test Methods for Analog to Digital Converters), and IEEE Standard 1057-1994 [2]. These two standards—especially the first one which is related exclusively to ADC converters—define the important characteristics of the state of the art in ADC measurements.

These standards specify several figures of merit for ADC characterization including nonlinear behavior. Tests similar to those carried out on radio transceivers have been developed, including characterization of nonlinear distortion through single, two-tone, and multisine excitation. However, when multisines are referred to, nothing is stated relative to their time-domain envelope characteristics.

Two different procedures take place in an ADC: time sampling of the signals and the quantization process. Both of

these can have a significant impact on the nonlinear behavior of the ADC [5-6]. Many authors consider that the sampling subsystem, or the so called sample-and-hold circuit, can be represented by a linear transfer function with dynamic characteristics [7]. Thus, sampling is often considered a second-order nonlinear effect.

The most important contribution to the output distortion comes from the quantization process, because this is an inherently nonlinear process. This process can generate a large amount of quantization noise. The analysis of quantization noise goes back several decades [8-9]. However, the characterization of nonlinear distortion in RF systems dates to 1981 with the work of Blachman [10]. In this work, the nonlinear generation of third-order harmonics at the output of an ADC is concisely studied.

Another aspect of distortion introduced in the quantization process is based on hard clipping of complex modulated waveforms. When the dynamic range of the ADC is exceeded, the output is strongly compressed. This also strongly impacts the generation of nonlinear distortion in ADCs [11].

In [12], the use of multisines in simulating broadband excitation was addressed. The work of Rabijns *et al.* [12] studies the purity of those multisines with regard to spectral distortion when testing low distortion ADCs, but nothing is discussed relative to the envelope PAPR.

Here, we study the effects of excitation PAPR on key nonlinear mechanisms in an ADC. Representative signals having a variety of distributions will be utilized and their impact on harmonic distortion and intermodulation distortion as analyzed from an ADC point of view follows the approach used in [13].

II. SOURCES OF NONLINEAR DISTORTION IN ADCS

As mentioned above, the sampling and quantization processes can generate nonlinear distortion in ADCs. While ADC manufacturers specify operating regions that minimize these effects, rapidly changing signals or transient excursions to high-power conditions can place the ADC into an unintended region of operation. Here, we illustrate these effects and describe how they manifest themselves in terms of nonlinear distortion.

Quantization changes a sine wave from a smooth function to a staircase signal, as illustrated in Figure 1(a). Due to this nonlinear effect, the output signal is composed of a large number of nonlinear distortion products. For instance, if a sine wave is used at the input, then the output will be the sine wave itself followed by all of its harmonics, which largely arise from the non-ideal quantization effects on the input signal. This effect occurs equally for any amplitude of the input signal, but the distortion reduces with increasing numbers of bits.

¹ Partial contribution of the U.S. government, not subject to copyright in the United States.

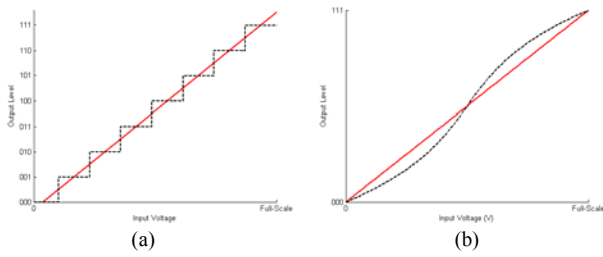


Figure 1: (a) Quantization of a continuous signal (solid) to discrete values (dashed). (b) Ideal ADC transfer function (solid) and non-monotonic ADC transfer function (dashed).

Another source of distortion common to ADCs relates to the maximum voltage that the ADC can digitize without clipping. If we overdrive the ADC transfer curve we will again generate harmonics of the input signal. This distortion is amplitude dependent and is of great importance in many new wireless communication systems, due to the high peak-to-average power ratio of their signals.

Finally, a third source of nonlinearity in an ADC is the non-monotonicity of its transfer function, as illustrated in Fig. 1(b). Non-monotonicity can be responsible for missing bits, and subsequent integral nonlinearity (INL) and differential nonlinearity (DNL)².

To aid in visualization, we can thus describe the ADC nonlinear behavior with a model similar to that in Fig. 2.

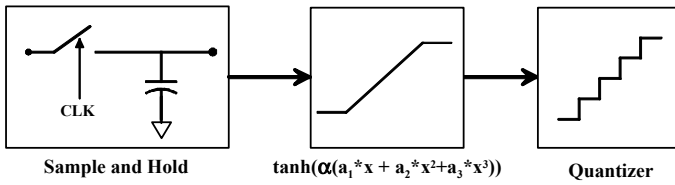


Figure 2: Behavioral model for describing key ADC nonlinear mechanisms. The highly nonlinear sampling process can often be represented as a linear but dynamic process. The sampler is followed by the nonmonotonic and finite-range transfer function of the ADC. Finally, the sampled signal is quantized.

This model is similar to previous solutions [5, 14], but here we consider clipping phenomena represented by the hyperbolic tangent function and a non-monotonic behavior represented by the polynomial argument of the clipping function. In this simple model, the polynomial parameters can be extracted by using small-signal measurements, based mainly on statistical measurements and DNL or INL results. The α parameter in the transfer function can be obtained from the reference voltage of the ADC (the maximum voltage before clipping).

When ADC nonlinear behavior is studied, most of the published works are found to be devoted to excitation signals consisting of one single sinusoid, two sinusoids, and more recently multisine signals that better represent real wireless communication signals. However, previous work does not describe the effect of the envelope on the ADC nonlinear behavior.

² INL is defined as the maximum difference between the ideal and actual code transition levels after correcting for gain and offset of the ADC, and DNL is defined as the difference between a specified code bin width and the average code bin width, divided by the average code bin width.

III. TWO-TONE AND MULTISINE MEASUREMENT RESULTS

We evaluated ADC nonlinear distortion through measurement. To synthesize the multisines, we used an arbitrary waveform generator (AWG) coupled to a vector signal generator. In order to reduce the distortion generated by the AWG, we used a high-power amplifier and operated it in a back-off mode. We measured the RF signal before the ADC, and the distortion was negligible.

The output signal was acquired by a logic analyzer and post-processed by a commercial mathematical software package. A clock generator was used to synchronize the instrumentation and trigger the waveforms.

The ADC used was a 12-bit, commercially available ADC with a clock frequency of 80 MHz and a maximum input frequency of 750 MHz. The carrier frequency was selected so that the ADC operated in a Nyquist-sampled or undersampled configuration.

We first carried out measurements using a two-tone excitation with a bandwidth of 1 MHz centered at different carrier frequencies. Figure 3(a) shows the output power of the upper fundamental tone, while Fig. 3(b) shows the power in the upper third-order intermodulation distortion product.

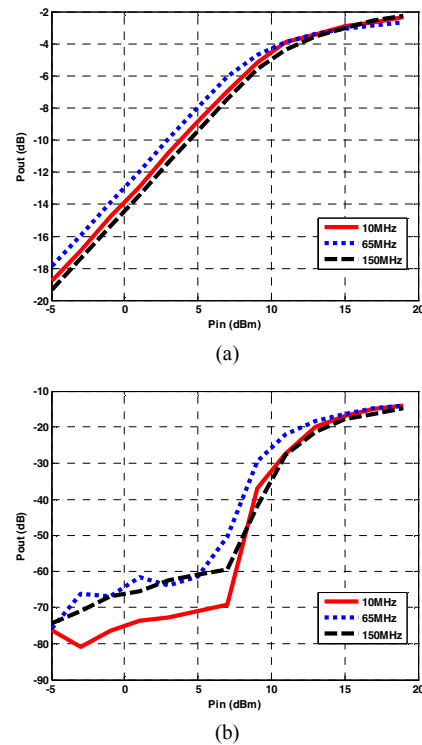


Figure 3: Two-tone ADC measurement for different carrier frequencies. The input power in the excitation signal is swept from -5 dBm to $+19$ dBm in 2 dB steps. (a) Output fundamental signal of the upper tone. (b) Power in the upper third-order intermodulation distortion product.

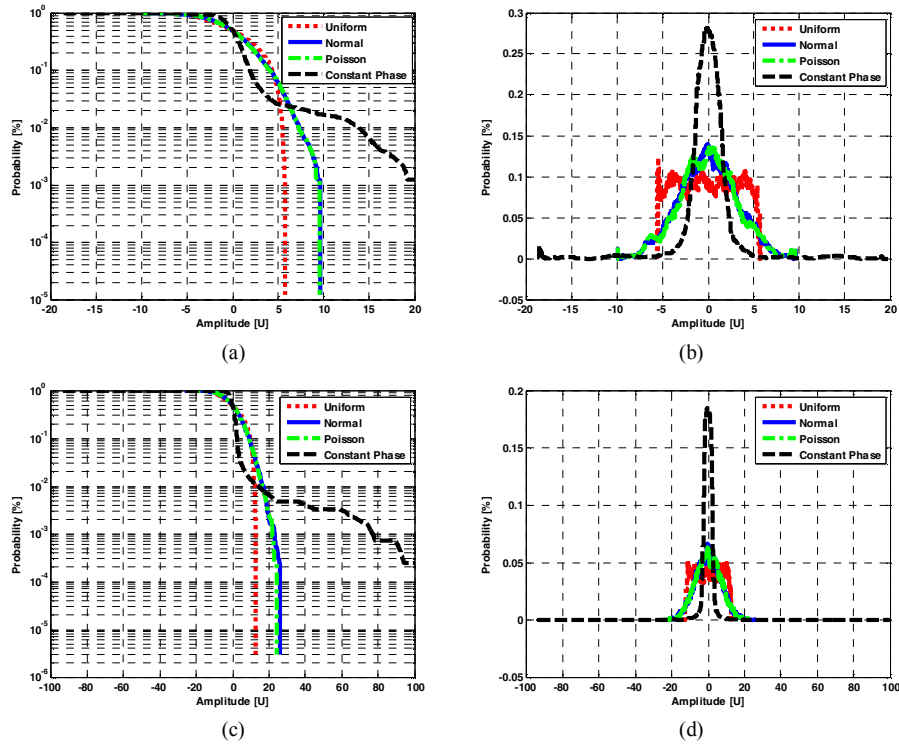


Figure 4: Measured signal statistics for different multisine excitations of 20 tones: (a) CCDF, (b) PDF and 100 tones: (c) CCDF, (d) PDF.

For small-signal behavior, we see that the power in the fundamental tone rises at approximately 1 dB per 1 dB increase of input power. This indicates that the nonlinear distortion we are measuring is due to input noise, which does not affect the linearity of the output signal because this noise is constant at all input levels. At high input power (near +11 dBm), the output compresses to a constant value. In this case, the nonlinear distortion is a combination of both quantization noise and clipping, where the clipping dominates, as can be seen by the increase in third-order intermodulation distortion. The two-tone tests allow us to set some distortion boundaries that we can compare to the multisine excitations.

Several amplitude/phase arrangements for the frequency components of the multisines were used in order to mimic different time-domain-signal statistics and thus PAPR. Here we show results for 20-tone and 100-tone multisines.

Table 1: PAPR (dB) for each excitation signal.

20 Tone Multisine		100 Tone Multisine	
Uniform	1.9	Uniform	2.15
Normal	6.7	Normal	8.25
Poisson	6.75	Poisson	7.75
Constant Phase	12.9	Constant Phase	19.9

Figure 4 and Table 1 present the measured statistics for each multisine arrangement. We intentionally used multisines with differing PAPRs. The *Constant Phase* arrangement is one where the relative phase difference was 0° between the tones. In the case of 100 tones this yields a large PAPR value of 20 dB. As can be seen from Fig. 4 and Table 1, the PAPR varies significantly with the number of tones and the engineered statistics of the multisine.

These multisines were then used as excitation signals for the 12-bit ADC. The power in the RF signal was swept from -5 dBm to $+19$ dBm (20-tone multisine case) and from -9 dBm to $+19$ dBm (100-tone multisine case), with a total occupied bandwidth of 1 MHz.

Figure 5 presents the measured results. The left graphs show the total power at the excitation frequencies, while the right graphs show the total power in the adjacent channel (adjacent channel power ratio, ACPR) arising from intermodulation distortion.

Again the small-signal behavior of the ADC is characterized mainly by the noise, as was seen in the two-tone case. The ACPR starts to rise for values where the output signal begins to approach the limits of the ADC. Figure 5 shows that the signal with constant-phase statistics does not compress for the range of input powers that we swept. The pdf of the constant-phase case (Fig. 4(d)) shows that for most of the envelope cycle the signal is concentrated around zero volt. Thus, even though the signal clips at a relatively low input level, ADC does not significantly compress until the input power is quite high. Also, the adjacent channel power is significantly higher for the constant-phase case than for the others.

Figure 5(b) shows that, for the 20-tone multisine, the ACPR distortion starts to increase when the input power is around -3 dBm for the *Constant Phase* case and near $+3$ dBm for the *Normal* and *Poisson* statistics. This is in perfect accordance with the PAPR difference for these statistical arrangements, $\Delta_{\text{PAPR}} = 6$ dB. The same can be seen for the *Uniform* case, where the ACPR starts to rise near $+7.5$ dBm, and $\Delta_{\text{PAPR}} = 11$ dB for this case. For the 100-tone case, similar results can be seen for the differences between the statistical behaviors.

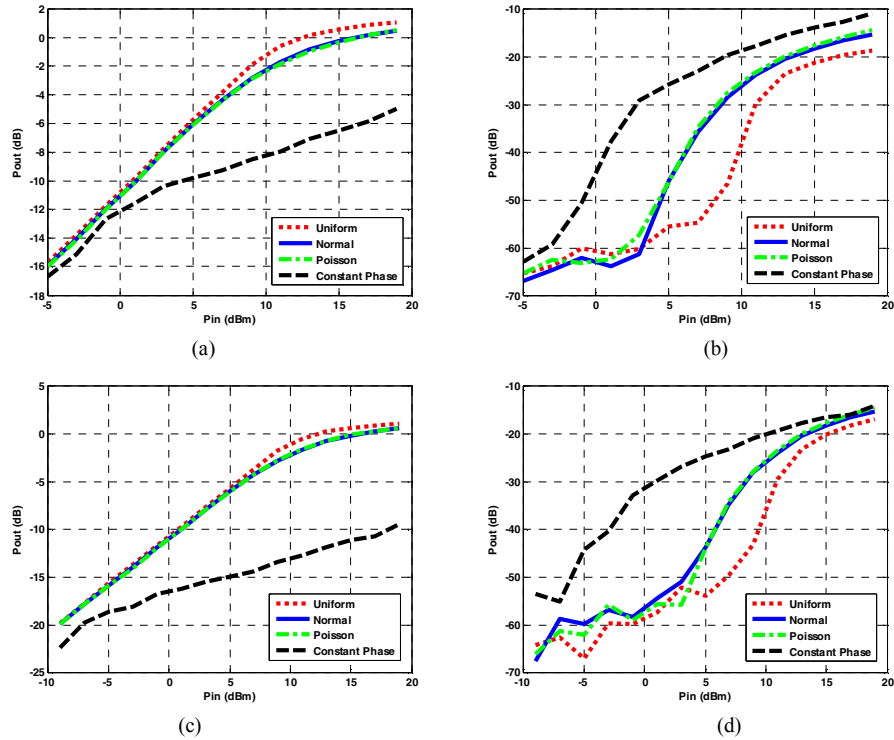


Figure 5: Measured output power for (a) 20 tones and (c) 100 tones; ACPR distortion for (b) 20 tones and (d) 100 tones.

IV. CONCLUSIONS

In this paper, we described measurements of the nonlinear distortion behavior of a typical commercial ADC for different excitation signals. These included two-tone and multisine input signals presenting different statistical arrangements. We developed a model that accounts for various nonlinear distortion mechanisms of ADCs.

Results of our study show that the small-signal distortion arises primarily from noise. We saw that the large-signal distortion is due mainly to clipping of the signal waveform. We were able to identify the link between the nonlinear distortion mechanisms and the types of distortion measured using different multisines with different PAPR.

REFERENCES

- [1] Waveform Measurement and Analysis Technical Committee of the IEEE Instrumentation and Measurement Society, "1241-2000-IEEE standard for terminology and test methods for analog-to-digital converters," *IEEE Standard*, 13 June 2001.
- [2] Waveform Measurement and Analysis Committee of the IEEE Instrumentation and Measurement Society, "1057-1994-IEEE standard for digitizing waveform recorders," *IEEE Standard*, 30 Dec. 1994.
- [3] N. Nagi, J.A. Abraham, "Test trade-offs for different dynamic testing techniques for analog and mixed-signal circuits," *Proc. Economics of Design, Test, and Manufacturing*, 1994, May 16-17, 1994, pp. 142.
- [4] N. Vun, A.B. Premkumar, "ADC systems for SDR digital front-end," *Intl. Symp. Consumer Electronics (ISCE 2005)*, June 14-16, 2005, pp. 359-363.
- [5] P. Arpaia, P. Daponte, and S. Rapuano, "A state of the art on ADC modeling," *Comput. Standards Interfaces*, vol. 26, pp. 31-42, 2003.

- [6] P.A. Traverso, D. Mirri, G. Pasini, F. Filicori, "A nonlinear dynamic S/H-ADC device model based on a modified Volterra series: identification procedure and commercial CAD tool implementation," *IEEE Trans. Instrum. Meas.*, vol. 52, no. 4, Aug. 2003, pp. 1129-1135.
- [7] G. Vandersteen, Y. Rolain, J. Schoukens, "An identification technique for data acquisition characterization in the presence of nonlinear distortions and time base distortions," *IEEE Trans. Instrum. Meas.*, vol. 50, no. 5, Oct. 2001, pp. 1355-1363.
- [8] B. Widrow, "A study of rough amplitude quantization by means of Nyquist sampling theory," *Trans. IRE*, vol. 3, no. 4, Dec. 1956, pp. 266-276.
- [9] Bennett, W. R. "Spectra of 'Quantized Signals,'" *Bell System Technical Journal*, vol. 27 (July, 1948) p. 446-472.
- [10] N. Blachman, "Third-Order intermodulation due to quantization," *IEEE Trans. Comm.*, vol. 29, no. 9, Sept. 1981, pp. 1386-1389.
- [11] D. Dardari, "Joint clip and quantization effects characterization in OFDM receivers," *IEEE Trans. Circ. and Syst. I: Regular Papers*, vol. 53, no. 8, Aug. 2006, pp. 1741-1748.
- [12] D. Rabijs, W. Van Moer, G. Vandersteen, "Using multisines to measure state-of-the-art analog-to-digital converters," *IEEE Trans. Instrum.Meas.*, vol. 56, no. 3, June 2007, pp. 1012-1017.
- [13] K.A. Remley, "Multisine excitation for ACPR measurements," *IEEE MTT-S Int. Microwave Symp. Dig.*, vol. 3, June 8-13, 2003, pp. 2141-2144.
- [14] J. Tsimbinos and K.V. Lever, "Applications of higher-order statistics to modelling, identification and cancellation of nonlinear distortion in high-speed samplers and analogue-to-digital converters using the Volterra and Wiener models," *IEEE Signal Processing Workshop on Higher-Order Statistics*, 1993, pp. 379-383.